 doi:10.20944/preprints202210.0433.v1

Article

The Wave Reduction Efficiency How Relates with the Crest Widths, Working States of Pile-rock Breakwater in Coastal Mekong Delta

Nguyet-Minh Nguyen [1], Duong Do Van [1], Tu Le Duy [1], Nhat Truong Pham [2,3], Thanh Duc Dang [4], Ahad Hasan Tanim [5], David Wright [6], Phong Nguyen Thanh [7,8] and Duong Tran Anh [7,8*]

[1]Southern Institute of Water Resources Research, Ho Chi Minh city, Vietnam; minh.nguyen.hus@gmail.com, DuongDV25@wru.vn, le.duytu0801@gmail.com
[2]Division of Computational Mechatronics, Institute for Computational Science, Ton Duc Thang University, Ho Chi Minh City, Vietnam; phamnhattruong.skyo@gmail.com
[3]Faculty of Electrical and Electronics Engineering, Ton Duc Thang University, Ho Chi Minh City, Vietnam; phamnhattruong.skyo@gmail.com
[4]Department of Civil and Environmental Engineering, University of South Florida, Tampa, FL, USA 33620; ddt21@usf.edu
[5]Department of Civil and Environmental Engineering, University of South Carolina, SC 29208, USA; ahtanim1001001@gmail.com
[6]Independent Researcher, Melbourne, Australia; david.wright.hydro@gmail.com
[7]Laboratory of Environmental Sciences and Climate Change, Institute for Computational Science and Artificial Intelligence, Van Lang University, Ho Chi Minh City, Vietnam; phong.nguyenthanh@vlu.edu.vn, duong.trananh@vlu.edu.vn
[8]Faculty of Environment, Van Lang University, Ho Chi Minh City, Vietnam; phong.nguyenthanh@vlu.edu.vn, duong.trananh@vlu.edu.vn
*Correspondence: duong.trananh@vlu.edu.vn

Abstract: The coastline in Ca Mau and Kien Giang provinces of the Vietnamese Mekong Delta has been severely eroded in recent decades. The Pile-Rock Breakwater (PRBW) was chosen as the predominant breakwater structure for controlling shoreline erosion. This structure shows the effectiveness of wave energy dissipation, stimulating sediment accumulation and facilitating the restoration of mangrove forests. However, this breakwater had been designed on the basis of best-engineering practice, lacking sufficient scientific evidences with regard to the structural design aspects, the effectiveness of the PRBW has compromised in the field scale implementation. This study investigates the PRBW design parameter, including crest width and working states (submerged, transition, and emerged), with their relationship with the wave transmission coefficient, wave reflection coefficient, and wave energy dissipation of PRBW by developing a physical model in the Laboratory. Further, the empirical formulas are derived for PRBW under different sea states and crest widths to aid the design process. The results show a significant influence of PRBW width on the wave energy coefficients. The findings revealed that the crest width of the breakwater is inversely proportional to the wave transmission coefficient (K_t) under emerged state. The crest width is also proportional to the wave reduction efficiency and wave energy dissipation in both working states, i.e., submerged and emerged states. The front wave disturbance coefficient (K_f) is proportional to the wave reflection coefficient, and the wave height in front of the structure can increase by 1.4 times in the emerged state. In order to reduce the toe erosion in the structure, the wave reflection coefficient requires special consideration. Lastly, the empirical equations including linear and non-linear formulas have also developed and compared with previous studies for different breakwaters. The empirical equations are useful for understanding the wave transmission efficiency. The findings of this study could serve as a powerful basis for PRBW design in the coastal area of the Mekong Delta.

Keywords: pile-rock breakwater; wave transmission; wave reflection; energy dissipation; physical model; East Sea of Mekong Delta

1. Introduction

Shoreline erosion in the Mekong Delta has been rapidly accelerating in recent decades at both spatial and temporal scales. The complexity of driving forces for shoreline erosion is broadly researched, but reducing the wave efficiency as the main driver for shoreline protection has sparked debates in the scientific community, particularly for deltaic coasts, because sedimentation is required for the living shoreline. However, it should be acknowledged that the sediment reduction in the Vietnamese Mekong Delta (VMD) due to upstream dam construction has been studied extensively, which also contributes to shoreline erosion of the Mekong delta [Error! Reference source not found.-Error! Reference source not found.]. Moreover, other driving forces, including changing wind wave climatology with climate change, sea level rise, sand mining, and land subsidence due to over-extraction of groundwater, have exacerbated the shoreline erosion in Mekong Delta [Error! Reference source not found.-Error! Reference source not found.]. Specifically, Ca Mau and Kien Giang have experienced a relatively higher rate of erosion. Therefore, several pilot projects were implemented to adopt different types of breakwaters to protect the Ca Mau coast, such as geotube, non-metallic reinforced hollow breakwaters, hollow cylinder, and pile-rock breakwaters [Error! Reference source not found.-Error! Reference source not found.]. Among them, the pile-rock breakwater (PRBW) shows significant advantages in terms of wave reduction, stimulating sedimentation, mangrove restoration, and stability under strong waves condition during monsoon season (Error! Reference source not found.).

Figure 1. The pile-rock breakwater was constructed in the west sea of the Mekong Delta.

Over a ten-year period of observation, PRBW is widely adopted because easily manageable and low-cost maintenance support breakwaters from a practical engineering point of view. For example, this structure is suitable for soft soil foundation conditions, stable seabed protection against scouring, and is highly effective for wave energy dissipation [Error! Reference source not found.]. The porous medium created by filling the PRBW structure with rocks allows fine-grained sediments to pass through, stimulating onshore sedimentation and helping to restore the mangrove forest (Error! Reference source not found.). Presently, this structure is widely constructed on the Mekong coast at a stretch of 70 km in length, particularly at Ca Mau and Kien Giang at about 65 km. There are many locations being recovered for mangrove forestation in the west sea in Ca Mau province because of the established performance of PRBW in terms of wave reduction and sedimentation [Error! Reference source not found.-Error! Reference source not found.].

Preprints (www.preprints.org) | NOT PEER-REVIEWED | Posted: 27 October 2022 doi:10.20944/preprints202210.0433.v1

However, this breakwater had been designed on the basis of best-engineering experience, lacking sufficient scientific background with regard to the structural design, stability, capacity of wave reduction, and optimal percentage of porosity. In spite of having current standards such as TCVN 9901:2014 or TCVN 12261:2018, these are not complete in all design aspects. There were many construction challenges faced during the PRBW construction on the west coast of the Mekong Delta. For instance, no design guidelines for the crest width and height of PRBW are available.

There were few studies conducted based on the effectiveness of PRBW in terms of wave reduction and sedimentation. For instance, Nhan [Error! Reference source not found.] employed numerical modeling with MIKE21/3 coupled model FM with hydrodynamic and sediment transport modules to simulate two-dimensional hydrodynamic and wave actions on a 300 m long PRBW shore but did not consider the details of the structural design, the processes of the waves overtopping, or wave transmission through the structure in numerical modeling. PRBW design in analytical and numerical analysis mainly focuses on stability without considering the crest width and working states (submerged, transition, and emerged). The previously mentioned results from numerical modeling were not justified with lab experiment data yet. Furthermore, Hur [17] and Hur et al. [Error! Reference source not found.] investigated the effect of the slope gradient of submerged breakwaters by using a three-dimensional numerical model setup and three-dimensional wave basin experiments. Recently, Le Xuan et al. [Error! Reference source not found.] tested the efficiency of PRBW with regard to wave transmission, wave reflection, and energy dissipation and constructed the empirical formula using experimental results from the Laboratory. A wide range of working states (water level and crest freeboard) and incident wave conditions were tested to build an empirical formula using the fixed crest width of PRBW. However, those studies have not investigated the variation of crest width with respect to the wave transmission coefficient, wave reflection coefficient, and wave energy dissipation.

A numerical modeling study was also done to investigate wave propagation through porous breakwaters. Tsai et al. [Error! Reference source not found.] developed a numerical model for testing the submerged permeable breakwater efficiency for wave energy dissipation. The wave propagation can be deduced by deriving governing equation based on the linearized equation of unsteady flow in a porous medium. Experimental results show that the waves started decaying in front of the breakwater, then decreased rapidly over the breakwater, and the decay process interfered with its way of wave transmission due to the permeability and resistance of the porous medium. Lin & Karunarathna [Error! Reference source not found.] investigated the solitary wave interaction with porous breakwaters using a two-dimensional numerical model using the Reynolds-averaged Navier-Stokes equations. The effect of porous media in the model simulation was considered by adding inertia and drag forces according to Morison's equation, assuming uniform spherical particles. The model was employed to study solitary wave interaction with fully emerged porous rectangular breakwaters. Paradoxically, the wave reflection coefficient was higher than that predicted by the theory in the case of large permeability. The probable reason for this deviation could be the linearization of friction terms in theory.

Zhang et al. [Error! Reference source not found.] also developed a new model using Reynolds-Averaged Navier–Stokes equations to investigate the mechanism of the wave–permeable porous structure for understanding changes in bed morphology. Higher wave height and longer wave periods led to higher pore pressure inside the breakwater. Increasing structural porosity content may reduce the pores pressure on the lee side of the breakwater. The seabed thickness, soil permeability, and degree of saturation could also significantly affect the dynamic soil behavior. Remarkably, Wu & Hsiao [Error! Reference source not found.] studied the interaction of a solitary wave and a submerged permeable breakwater by both experimental and numerical modeling. They suggested that the maximum turbulent intensity usually occurs at the front side and top corner of the breakwater. The energy reflection coefficients are dominated by the porosity and decrease with increasing porosity. The crest width of the submerged breakwater has significant effects on the energy transmission and dissipation coefficients. As the crest width of the breakwater increases, the energy transmission coefficients decrease, and the energy dissipation coefficients increase. These conclusions were confirmed by Wu et al. [Error! Reference source not found.] applying a three-dimensional numerical model to examine the interaction of solitary waves and porous breakwaters. Considering the knowledge gap of the breakwater width and crest width, how can improve the breakwater efficiency in terms of wave energy dissipation, the objectives of this study are to investigate the relationship between the crest width, working states (submerged, transition and emerged) of PRBW with three wave energy coefficients, i.e., the wave transmission, wave reflection, and energy dissipation by developing physical models in laboratory. Moreover, the empirical formulas also developed to deliver linear and non-linear equation that can be applied for PRBW in the West coast of the Mekong Delta.

This paper is structured as follows. In Section 2, we describe the experimental setup and results of investigating wave transmission through a PRBW based on observations in the Laboratory. Section 3 describes the result and discussion of experimental analysis and development of empirical formulas and comparison of wave transmission coefficient by different equations for three types of breakwaters. Finally, in Section 4, we make conclusions from both the laboratory experiments as well as the numerical modeling and provide recommendations for future work.

2. Laboratory experiments

2.1. Experiment equipment setup

The experiment was carried out in the wave flume of the Marine Hydrodynamics Laboratory- located at the Southern Institute of Water Resources Research (**Error! Reference source not found.**a) in 2021. Required experimental equipment was provided by HR Wallingford (UK). The length of the wave flume is 35 m, the width is 1.2 m, and the height is 1.5 m. The wave generator system is equipped with the ability to absorb reflected waves (Active Reflection Compensation). The wave generator can generate random or uniform waves with a height of up to 0.30 m and a peak period of 3.0s. Waves are measured using many wave gauges with a frequency of 50Hz (accuracy ±0.1mm). Additional descriptions of the experimental wave flume setup are detailed in Le Xuan et al. [11]. In this experiment, the wave-absorbing is set at the end of the wave flume, using aluminum slag material placed in an iron cage with a slope of 1/5 (**Error! Reference source not found.**b). The validation results of the wave absorber for all test cases (change of water level, wave parameters) show that the waves reflected from the absorber are less than 10%.

The physical model scale was selected to ensure both technical considerations and economic resource utilization. The larger model ratio usually leads to higher reliability of the experiment. However, large-scale physical model sets up are expensive. We selected the model ratio based on wave flume capacity and satisfying the hydrodynamic boundary conditions (waves, optimum water level). The model scale also ensures the similarity of Froude numbers and the turbulent flow in the flume, i.e., ([Reynolds Number, Re] > 10^4). The laboratory model was set up following Froude's law to ensure turbulent hydrodynamic conditions. The model scale was selected as the following: N_L=7 (scale of length and height), $N_t = \sqrt{N_l} = 2.64$ (scale of time), $N_v = \sqrt{N_l} = 2.64$ (scale of velocity), and $N_m = N_L^3 = 343$ (scale of mass). The size of the rock for the experiment also ensures the flow condition through the rock layer as much as remains turbulent with [Re] > 10^4 according to the formula:

$$R_e = \frac{\rho v D}{\varepsilon \mu} \quad (1)$$

Where v is the wave velocity flowing through the hole, D is the diameter of the rock, μ is the absolute viscosity of the water (0.001002 Kg/ms), ε is the porosity of the rocks layer for the experiment ($\varepsilon = 0.4$). Based on the dimensional analysis, the Reynolds number of *Re* = 20,559 (Re> [Re]) satisfies the minimum velocity by the lowest waves amplitude under the most extreme case as well as the smallest diameter of rocks corresponding to Re that ensures the turbulent flow condition through the rock layer.

Preprints (www.preprints.org) | NOT PEER-REVIEWED | Posted: 27 October 2022 doi:10.20944/preprints202210.0433.v1

Figure 2. The wave flume house (a) and absorber at the lee side of wave flume (b).

2.2. Installation of equipment and model setup

The experimental model employs a wave transition zone, an inclined face having a slope of 1/25. It is 3 m far from the wave generator and 5 m towards the breakwater direction (Fig. 3). The transition zone propagates waves from deep waves to shallow waves simulating the nearshore topography along the Mekong Delta coast. (**Error! Reference source not found.**, bottom panel).

Five wave gauges were installed in front and behind the breakwater, including WG1, WG2, WG3, WG4, and WG5 on the seaside to measure the incoming wave, and two wave gauges (WG6, WG7) on the lee side to measure transmitted waves through the breakwater. Four-wave gauges, WG1, WG2, WG3, and WG4 were installed to detect the reflected and incident waves using the method of least squares. In addition, for measuring the current E40 probe is used in combination with the wave gauge at the same position as WG5 (**Error! Reference source not found.**).

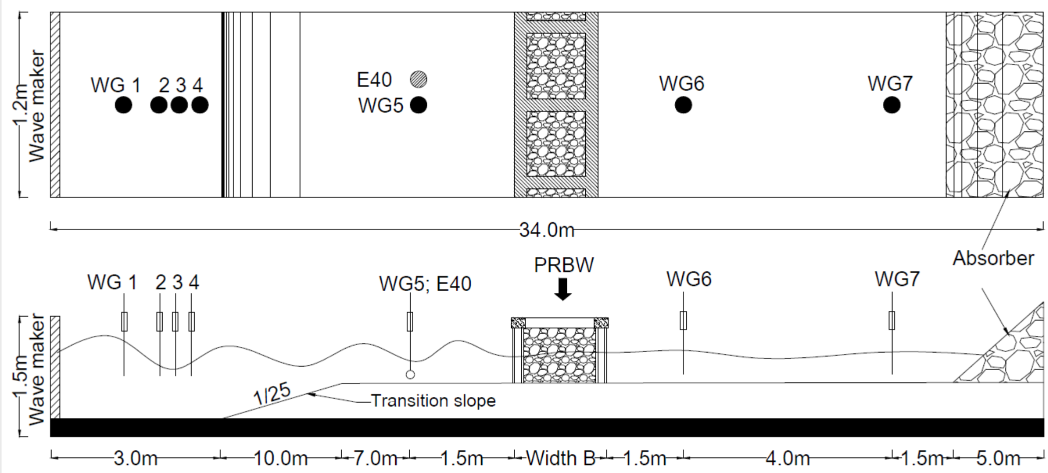

Figure 3. Sketch of experimental layout and equipment installation in the wave flume (diagram is not to scale).

Preprints (www.preprints.org) | NOT PEER-REVIEWED | Posted: 27 October 2022 doi:10.20944/preprints202210.0433.v1

The structure and dimensions of the typical PRBW in the Mekong Delta have a crest width of 2.5 m and a crest elevation of 1.6 m. PRBW are cast with pre-stressed concrete piles with a diameter of 0.30 m having a length of 8 m, as shown in **Error! Reference source not found.**. In this experiment, the structure of the centrifugal piles is linked with overhead beams in the physical model. The casings are made of wood to ensure the convenience of fitting inside the flume and high precision of components dimensions (**Error! Reference source not found.**). The rocks were selected having effective diameters of 4 – 7 cm to ensure the shape didn't turn too flat or too thin. The edges of rocks are relatively even and rough. The rock edges affect the friction of the surface of the rock. After sieving the rocks, the required volume method was implemented to determine the porosity of the rocks and mix them according to proportion. The porosity of the physical model was about P= 40%.

Table 1. Actual construction and experimental model dimensions.

Dimension	Scenarios	Actual (cm)	Model (cm)
Height		280	40
Length			120
Width (B)	B24	170	24
	B38	270	38
	B52	370	52
Rock mix		30-50	4-7
Centrifugal pile diameter		30	4

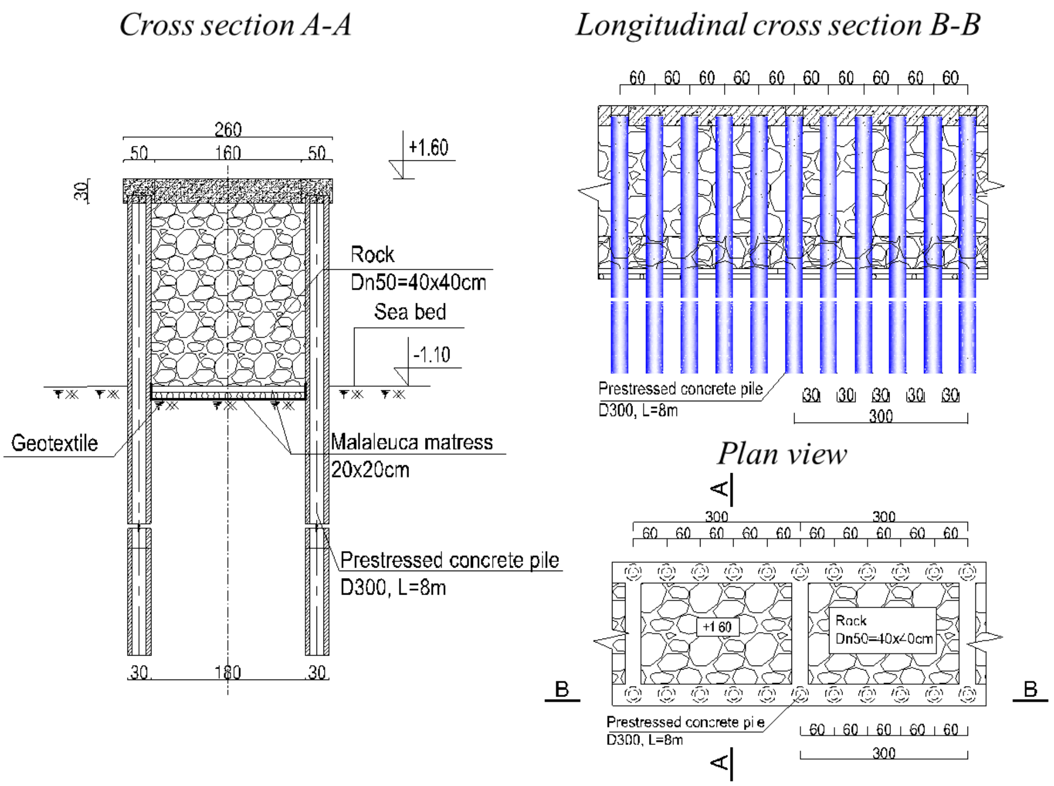

Figure 4. Cross-section, longitudinal, and plan view and dimensions of the Pile-Rock Breakwater (units: cm).

Preprints (www.preprints.org) | NOT PEER-REVIEWED | Posted: 27 October 2022 doi:10.20944/preprints202210.0433.v1

Figure 5. Experimental pile-rock breakwater set up in the wave flume at Laboratory.

2.3. Experimental scenarios

2.3.1. Wave conditions

The PRBW was designed for monsoon conditions. The input wave parameters were selected from in situ-measurement data and simulation results of a numerical model. The typical wave height for the Mekong Delta is a range between 0.5m - 1.5m, and a wave period (Tp) varies between 3s to 7s. The model scale N_L=1/7 is selected, so that wave height should be greater than or equal to 5 cm and maximum height do not exceed over 30cm. Minimum Tp is maintained greater than or equal to 1s so that waves don't exceed wave flume capacity, and maximum Tp is 3s to ensure precision in the calculation. To confirm that the experimental wave spectrum shape is consistent with the field case and to collect enough experimental set of data for analysis, each experiment was run for a duration of 500*Tp (s). The generated wave's frequency range is calculated to lie between 0.01 Hz and 1.5 Hz with a split of 0.01 s/value.

2.3.2. Experimental structures

PRBW was tested with three crest widths of 24cm (B24); 38cm (B38), and 52cm (B52) (**Error! Reference source not found.**), corresponding to the actual crest built in the Mekong Delta of 1.7m, 2.7m, and 3.7m. In order to better understand the relationship between the crest width, working states (submerged, transitional, and emerged), and the wave transmission, wave reflection, and energy dissipation of PRBW, we fixed additional dimensions such as height, rock distribution, distance, and diameter between centrifuge piles per row based on the field scale.

.

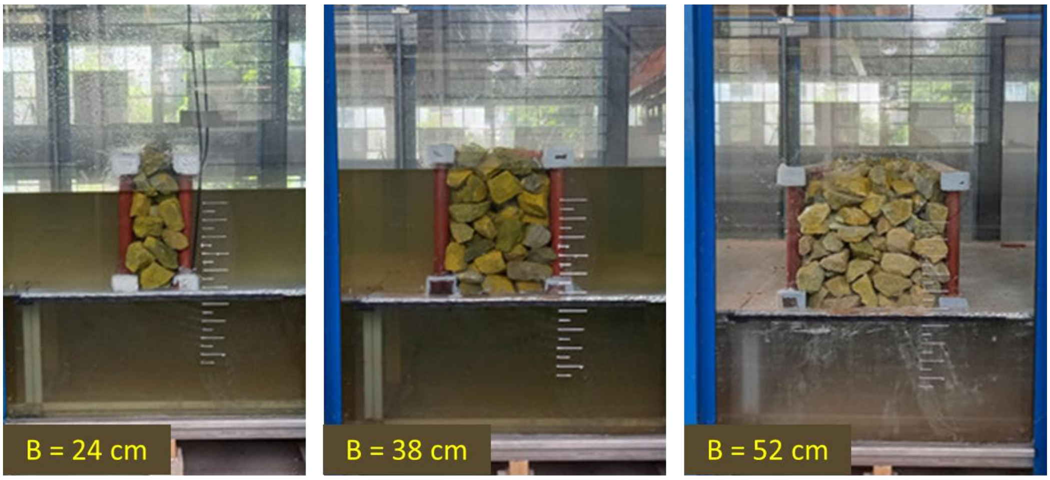

Figure 6. Width of the dike structure of centrifugal piles - poured rock in the experimental scenarios.

Preprints (www.preprints.org) | NOT PEER-REVIEWED | Posted: 27 October 2022 doi:10.20944/preprints202210.0433.v1

2.3.3. Testing scenarios

To investigate the relationship between the crest widths, working states (submerged, transition, and emerged), and the wave transmission, wave reflection, and energy dissipation of PRBW, there were large numbers of scenarios implemented to test with different sea states and crest widths. The experimental scenarios are shown in detail in **Error! Reference source not found.**. There are 280 experiment tests, including (Table 2):

- 1 test without PRBW and three tests with three crest widths (B24, B38, and B52);
- 07 tests of changing water level and crest freeboard (R_c);
- Changing ten parameters of wave (H_s, T_p, L);

Table 2. Experimental scenarios of different crest widths, water depths, and wave parameters.

Scenarios		Water depth D (cm) corresponding to crest freeboard R_c (cm)		Wave parameters
No PRBW B24 B38 B52	×	D=20cm (R_c=+20 cm) D=25cm (R_c=+15 cm) D=30cm (R_c=+10 cm) D=35cm (R_c=+5.0 cm) D=40cm (R_c=+0.0 cm) D=45cm (R_c=-5.0 cm) D=50cm (R_c=-10 cm)	×	H_s=12cm; T_p=1.51s H_s =12cm; T_p =1.89s H_s =12cm; T_p =2.27s H_s =12cm; T_p =2.65s H_s =17cm; T_p =1.89s H_s =17cm; T_p =2.27s H_s =17cm; T_p =2.65s H_s =22cm; T_p =2.27s H_s =22cm; T_p =2.65s H_s =27cm; T_p =2.65s

3. Results and discussion

3.1. Wave spectrum validation

During wave propagation, in the transition zone from deep to shallow water, there are significant changes in water depth. Wave breaking happens in the transition zone. After breaking at the transition zone, the wave continues to propagate into the shallow water in front of the structure. The purpose of creating the transition zone is to force the wave to break many times, creating an incident wave condition in front of the structure with a similar wave energy spectrum as on the nearshore of the Mekong Delta.

The changes in the wave spectrum through the transition zone are shown in **Error! Reference source not found.**. From the deep-water zone (wave gauge WG1), the wave spectrum has a sharp peak with an energy value of 0.023 m^2/Hz (**Error! Reference source not found.**a), and through the transition zone, the spectral peak energy was significantly reduced to 0.011 m^2/Hz at wave gauge WG5. After wave breaking, the spectrum has transformed to a flattened shape with many low peaks (**Error! Reference source not found.**b). Thus, the energy decreased significantly due to wave breaking.

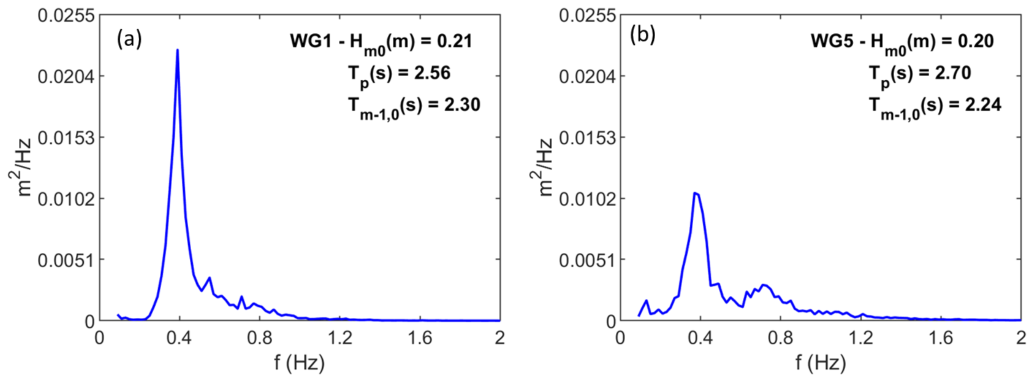

Figure 7. Wave spectrum in front of and behind the transition slope face at wave gauge WG1 (a) and WG5 (b).

The wave spectrum generated in the model after passing through the transition zone was also compared to the actual pattern observed in the field at Ganh Hao coast, Bac Lieu. In the typical shallow water condition of the Mekong Delta, the similarity of wave spectrums between the field observation and physical model is shown in **Error! Reference source not found.**. The wave spectrums in both locations were flattened and scattered to multi-peaked values. In the case of field observation, high-energy peaks are in the middle, and small peaks are on either side in the frequency bands. The wave spectrum from the physical model confirms that it has simulated the field wave conditions in order to increase the reliability in the study of wave interaction on the breakwater.

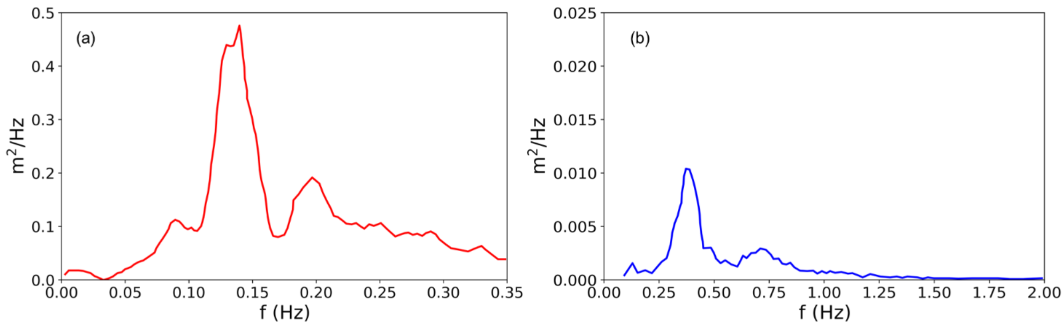

Figure 8. Wave spectrum from observation at Ganh Hao coast in 2019 (a) and experiment (b).

3.2. Experimental analysis

Incident wave train, water level, crest freeboard, and crest widths with a total of 280 experimental scenarios are tested. A typical sketch of the experiment of wave propagation on the PRBW is shown in **Error! Reference source not found.**.

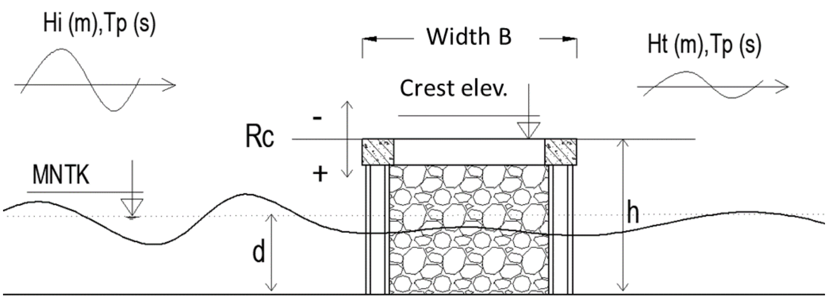

Figure 9. The sketch of the experiment of wave propagation on the PRBW.

Preprints (www.preprints.org) | NOT PEER-REVIEWED | Posted: 27 October 2022 doi:10.20944/preprints202210.0433.v1

The structure of PRBW is a porous media as vertical seawall construction. The distance between the centrifugal piles and the porosity of the filling rocks have affected the ability of wave energy dissipation and reflection. According to the law of conservation of energy, the energy can be expressed mathematically using the energy balance formula Van der Meer & Daemen [24]:

$$E_i = E_t + E_r + E_d \tag{2}$$

Where, E_i, E_t, E_r, and E_d are the energies of the incoming wave, the transmitted wave, the reflected wave, and the dissipated wave, respectively. From this, the energy balance function can be rewritten as:

$$1 = \left(\frac{H_t}{H_i}\right)^2 + \left(\frac{H_r}{H_i}\right)^2 + \frac{E_d}{E_i} \tag{3}$$

$$1 = K_t^2 + K_r^2 + K_d \tag{4}$$

Where:

$K_t = \frac{H_{m0,t}}{H_{m0,i}}$ The wave transmission coefficient is determined by the ratio of the wave height behind the breakwater ($H_{m0,t}$) and the wave height in front of the breakwater ($H_{m0,i}$);

$K_r = \frac{H_{m0,r}}{H_{m0,i}}$ The reflected wave coefficient is determined by the ratio of the reflected wave height in front of the breakwater ($H_{m0,r}$) and the wave height in front of the breakwater ($H_{m0,i}$);

K_d is determined based on the transformation from the formula (3):

$$K_d = 1 - K_t^2 - K_r^2 \tag{5}$$

The front wave disturbance coefficient in front of the breakwater is determined by the difference in wave height at position WG5 with and without the structure:

$$K_f = \frac{H_{m0,i,bef}}{H_{m0,i,aft}} \tag{6}$$

3.2.1. The effect of crest width on the wave transmission coefficient

The PRBW works under three states including the submerged ($R_c < 0$), the transition ($R_c = 0$) and the emerged states ($R_c > 0$). The correlation between the relative crest freeboard ($R_c/H_{m0,i}$) and the wave transmission coefficient (K_t) through the PRBW is shown in **Error! Reference source not found.**. It can be seen that K_t ranges from 0.2 to 0.7 and is inversely proportional to the crest width (B) of PRBW. However, the curve tends to converge when the breakwater works under the submerged state ($R_c/H_{m0,i} \ll 0$). It demonstrates that the effect of crest width will decrease when PRBW works under the submerged state. When the PRBW works under the emerged state ($R_c/H_{m0,i} > 0$), the wave transmission coefficient decreases gradually when increasing R_c and when $R_c/H_{m0,i} > 1.5$, the reduction of K_t is not significant. On the other hand, the crest width of PRBW increases linearly with different widths from 24cm to 38cm and to 52cm, while the wave transmission coefficient decreases non-linearly, corresponding to the increase in crest width.

Error! Reference source not found. shows the wave transmission coefficient is the largest with $K_t = 0.4$ - 0.75 for the crest width of $B = 24$. Meanwhile, the wave transmission coefficients for $B = 38$ cm and $B = 52$ cm are similar with $K_t = 0.2$ - 0.65. This shows that when the crest width of the PRBW increases from $B = 24$ cm to $B = 38$ cm, the K_t reduces significantly from $K_t = 0.4$ to $K_t = 0.2$, corresponding to the emerged state, when the crest width continues to increase $B \geq 38$ cm corresponding to the actual width of the PRBW ≥ 1.7m, then the wave transmission coefficient changes insubstantially.

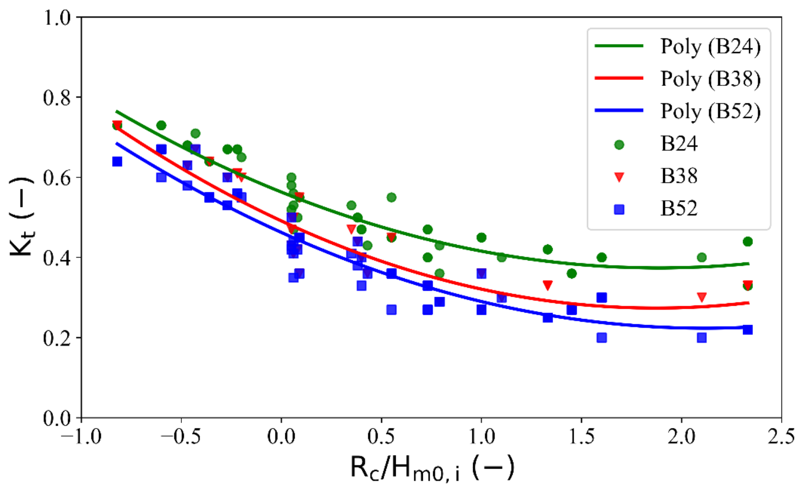

Figure 10. The relationship between relative crest freeboard ($R_c/H_{m0,i}$) and wave transmission coefficient (K_t).

The crest widths have affected the wave transmission coefficient (K_t) in all three working states (**Error! Reference source not found.**). In which the wave transmission coefficient in the submerged state changes slightly with wide ranges of the ratio of B/H_i (the blue curve is a small slope). The B/Hi ratio is inversely proportional to the wave transmission coefficient. The higher ratio of B/Hi corresponds to a lower transmission coefficient. In the emerging state, the wave transmission coefficient ranges from 0.2 to 0.45. In the transition state, the range of K_t varies from 0.35 to 0.6, and for the submerged state, K_t ranges from 0.55 to 0.75.

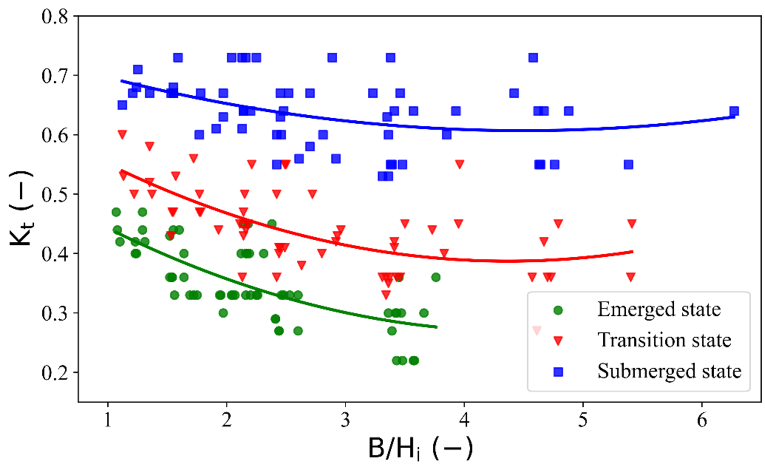

Figure 11. The relationship between B/H_i and wave transmission coefficient (K_t).

3.2.2. The effect of crest width on wave reflection coefficient

Error! Reference source not found. shows the relationship between the relative crest freeboard ($R_c/H_{m0,i}$) and wave reflection coefficient (K_r) for different crest widths. The wave reflection coefficients range from 0.15 to 0.45 in all cases of crest width. The wave reflected coefficient is proportional to the relative crest freeboard. However, the wave reflected coefficient fluctuates inconsiderably from 0.15 ÷ 0.25 when the PRBW works under a submerged state ($R_c/H_{m0,I} < 0$), but K_r alters remarkably from 0.2 - 0.45 when the PRBW works under emerged state ($R_c/H_{m0,i} > 0$). When increasing the crest width from B = 24 cm to B = 38 cm and B = 52 cm under the same conditions (waves, water level, type of rock used for the structure), the reflected wave coefficient between the three cases changes slightly. This demonstrates that the wave-reflected coefficient of PRBW is not significantly affected by the crest widths.

Preprints (www.preprints.org) | NOT PEER-REVIEWED | Posted: 27 October 2022 doi:10.20944/preprints202210.0433.v1

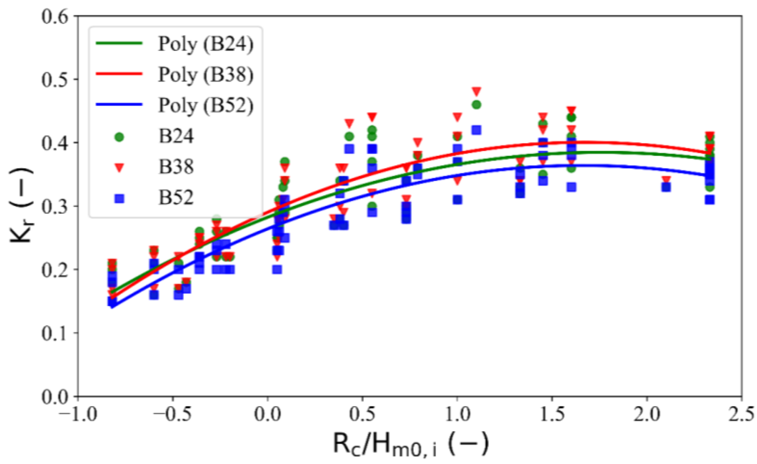

Figure 12. The relationship between relative crest freeboard ($R_c/H_{m0,i}$) and wave reflection coefficient (K_r).

The combination of reflected waves in front of the PRBW and the incoming waves through the process of interference and resonance creates the change in wave propagation on the PRBW. **Error! Reference source not found.** shows the increase in spectral peak energy in front of the PRBW. K_f is the front wave disturbance coefficient, which is the ratio of the wave height right in front of the breakwater to the incident wave height. The increase in spectral peak energy leads to a change in wave height in front of the structure, which can be increased by 1.4 times compared to the case without the structure, as described in **Error! Reference source not found.**, which is consistent with the study of Le Xuan et al. [11].

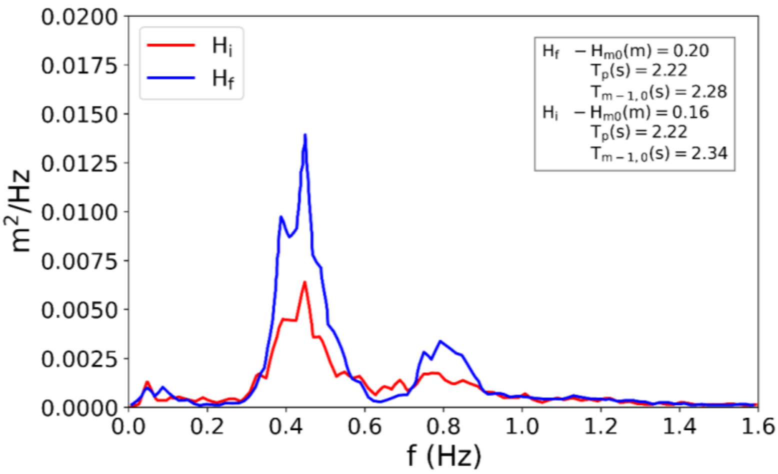

Figure 13. Front wave disturbance spectrum (H_f) and incident wave spectrum (H_i).

The incremental wave height in front of the PRBW is proportional to the relative crest freeboard ($R_c/H_{m0,i}$). When PRBW is still operating in the submerged state ($R_c/H_{m0,i} < 0$), the front wave disturbance coefficient is approximately one and increases gradually when the PRBW works under the transition state to the emerged state. The increment of the incoming wave disturbance coefficient (K_f) is due to the reflected wave in front of the structure, so the K_f is proportional to the reflected wave coefficient.

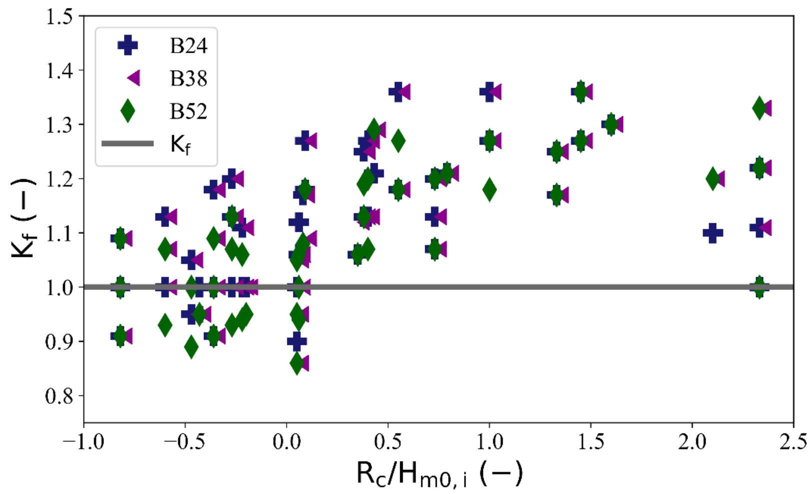

Figure 14. The relationship between front wave disturbance coefficient (K_f) and relative crest freeboard ($R_c/H_{m0,i}$).

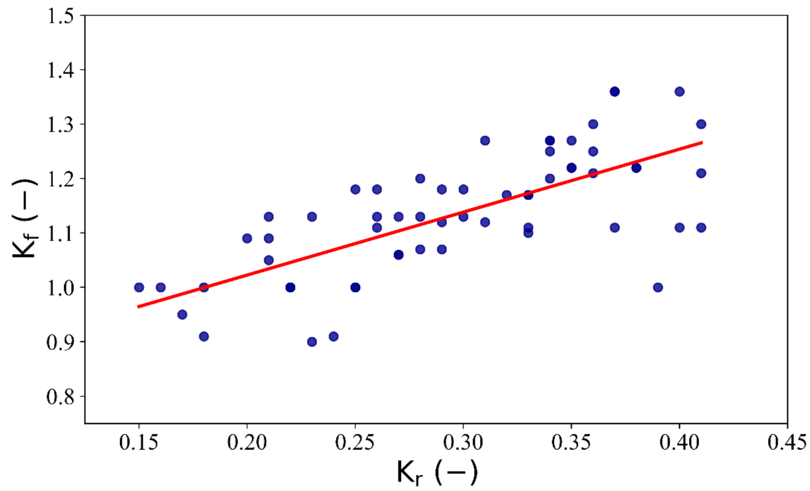

Figure 15. The relationship between wave reflection coefficient (K_r) and front wave disturbance coefficient (K_f).

3.2.3. The effect of crest width on energy dissipation

For the PRBW structure, the wave is dissipated by the process of passing through the piles of columns, the layer of rocks, and by friction with the rocks. The results show that the percentage of wave energy dissipated by the PRBW structure ranges from 40% to more than 80% of the incident wave energy. More wave energy is dissipated due to the larger the crest width; the maximum energy dissipation corresponds to the largest crest width (B = 52 cm) (**Error! Reference source not found.**). In the submerged state, when the relative crest freeboard is less than 0, the percentage of energy dissipation gradually increases from 40% to 70% for three crest widths. In the emerged state, when the relative crest freeboard is greater than 1, the dissipated wave energy tends to slightly increase and starts decreasing when $R_c/H_{m0,i} \geq 1.5$ for all cases. That means the dissipated energy only depends on the width and porosity of the PRBW.

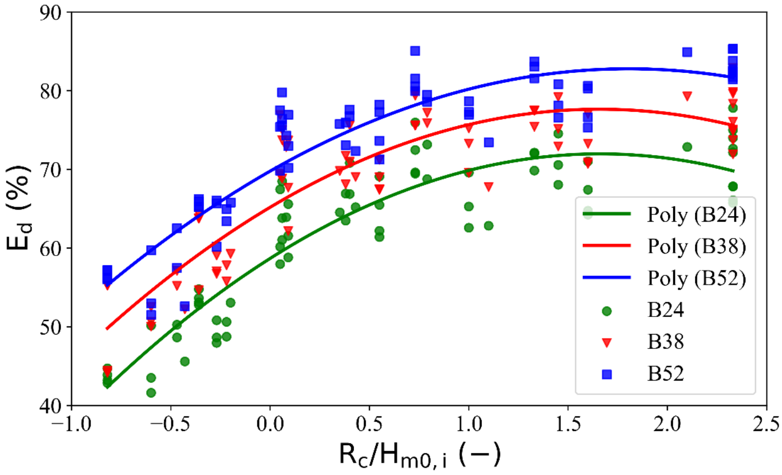

Figure 16. The relationship between relative crest freeboard ($R_c/H_{m0,i}$) and percentage of energy dissipation (E_d).

Error! Reference source not found. shows the average percentage of wave dissipation energy with the working states of the PRBW: submerged, transition, and emerged states with different crest widths. The average percentages of wave dissipation energy in transition and emerged states are superior to that of the submerged state.

The largest wave energy dissipation under the emerged state is approximately 70.35 - 81.47%, and the lowest dissipation energy in the submerged state is about 53.27 - 65.39%. However, in the case of the submerged state, the wave dissipation energy also increases with the expansion of crest width, with average values of about 53.27%, 60.64%, and 65.39% corresponding to the widths are B=24, B=38, and B=52cm, respectively. When the crest width of the PRBW increases by 14 cm, the wave dissipation energy of the structure increases by about 5% and obtains the maximum value of about 65.39%, corresponding to the maximum crest width under the submerged state.

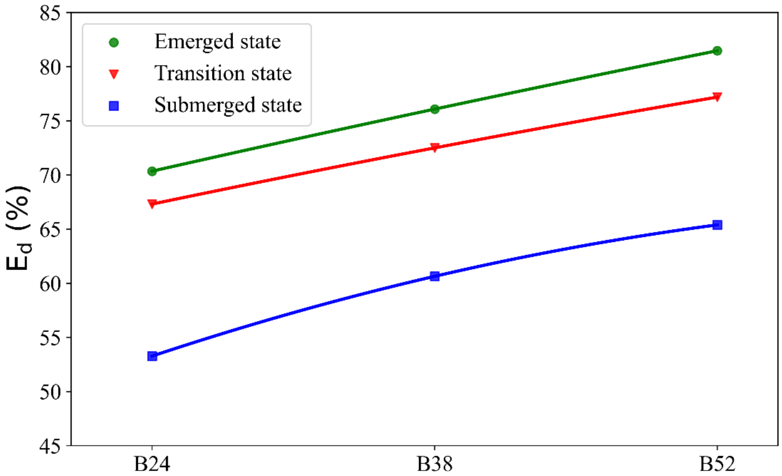

Figure 17. The relationship between crest width (B) and the average percentage of wave dissipation energy (E_d) at three working states of the breakwater.

3.3. Development of experimental equation for the wave transmission coefficient

The analysis of the parameters affecting wave propagation is the basis for building empirical formulas. This empirical formula is built based on several formulas developed by Van der Meer & Deamen [24], d'Angremond et al., [25] or Le Xuan et al. [11]. The general formula has the form:

$$K_t = F\left(\frac{R_c}{H_{m0,i}}, \frac{D}{L_m}, \frac{B}{D_{n50}}, S_{0p}\right) \tag{6}$$

From (6), we have evaluated the factors affecting K_t, including $R_c/H_{m0,i}$, D/L_m, B_n/D_{n50}, and S_{0p}. However, S_{0p} has insignificantly affected K_t, so we did not consider this factor when building the formula.

In order to cover a wide range of factors, we derive two empirical equations, including linear and non-linear equations.

$$K_t = a\frac{R_c}{H_{m0,i}} + b\frac{D}{L_m} + c\frac{B}{D_{n50}} + d \tag{7}$$

Where: a, b, c, d are the empirical constants characterizing the influence of the respective factors: Relative crest freeboard ($R_c/H_{m0,i}$), D/L_m, and (B/D_{n50}) to K_t.

a, b, c, and d are determined through the linear regression analysis method with data obtained from the experimental results.

The values a, b, c, and d are defined based on the maximum correlation coefficient R^2. For this linear equation, we obtained experimental data with R^2 = 0.82, as shown in **Error! Reference source not found.**a. The defined constants are: a = -0.1619; b = 0.4817, c = -0.0161 and d = 0.6284.

Substituting a, b, and c into (7), we have an empirical formula that determines the wave propagation coefficient:

$$K_t = -0.1619\frac{R_c}{H_{m0,i}} + 0.4817\frac{D}{L_m} - 0.0161\frac{B}{D_{n50}} + 0.6284 \tag{8}$$

The range of application of the formula is:

$-1.07 \le R_c/H_{m0,I} \le 1.98$

$0.413 \le D/L_m \le 0.191$

$4.2 \le B/D_{n50} \le 13.0$

For the non-linear equation, we have developed this equation with multiple independent variables, including crest width B. The equation is as follows:

$$K_t = a^*\left(\frac{H_{m0,i}}{B_n}\right)^{\alpha} + b^* \tag{9}$$

In which:

$$a^* = a + b\frac{R_c}{D_{n50}}\left(\frac{H_{m0,i}}{B_n}\right)^{1-\alpha}$$
$$b^* = c\left(\frac{H_{m0,i}}{D_{n50}}\right)^{\beta} + d\frac{D}{L_m} + e\frac{B}{D_{n50}} + f \tag{10}$$

The values a, b, c, d will be selected so that the correlation coefficient R^2 is highest (R^2 = 0.73) shown in **Error! Reference source not found.**b and the results of the constants are: a = 0.000363; b = -0.088, c = -2.641, d = 1.161, e = -0.033, f = 3.019, α = -3.70, and β = -0.1.

The range of application of the formula is:

$0.20 \le K_t \le 0.73$;

$-1.07 \le R_c/H_{m0,i} \le 1.98$

$-2.25 \le R_c/D_{n50} \le 5.25$

$0.16 \le H_{m0,i}/B \le 0.92$

$4.22 \le B/D_{n50} \le 13.00$

$1.12 \le H_{m0,i}/D_{n50} \le 5.52$

$0.041 \le D/L_m \le 0.191$

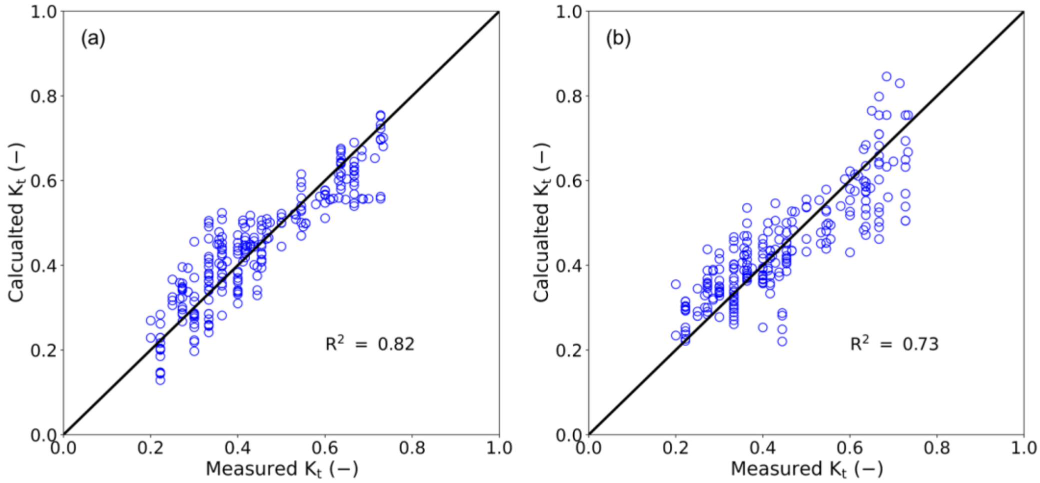

Figure 18. Regression analysis for a) linear and b) non-linear empirical equations.

3.4. Comparison of different empirical formulas for pile-rock breakwater

To evaluate the feasible application of different empirical formulas for pile-rock breakwater and verify our proposed equations, we have applied two empirical formulas developed by Angremond et al. [25] and Van Der Meer et al. [26] for pile-rock breakwater and we have compared the wave transmission coefficient (K_t) obtained from our empirical formulas with K_t calculated from three formulas obtained from previous studies including Le Xuan et al. [11], Tuan & Luan [27], and Tuan et al. [28]. We applied these empirical equations without any changes or adjustments of the parameters or equation and calculated K_t from these equations with our variables and wave conditions for pile-rock breakwater in this study. Because Tuan et al. [28] had built an empirical equation applied the formula from [25] for a perforated hollow breakwater to consider the surf similarity parameter or breaking wave Iribarren number ξ_0 but did not involve the crest width in the equation. Moreover, Tuan & Luan [27] employed the equation from [26] for bamboo fences in the Mekong delta. Le Xuan et al. [11] applied both empirical formulas from Van Der Meer and Daemen [24] and [25] for pile-rock breakwater but did not consider the variation of crest width.

We have evaluated our proposed formulas, including linear and non-linear equations, by comparing K_t from our study with those from [26, 25] in terms of the statistical performance, including adjusted R-squared (R^2), MSE, and RMSE. From

, it can be shown that for linear equations, the statistical indices are similar to those two previous formulas [24, 25].

Error! Reference source not found. shows a comparison between the wave transmission coefficients (K_t) against $Rc/H_{m0,i}$ for the case of Linear equation, Non-linear equation and comparison with K_t calculated from [26] and [25]. It can be seen that there is good agreement between the K_t from the empirical formula and experiment data shown in **Error! Reference source not found.**a,b. In addition, the trend from linear and non-linear equations is consistent with the trend of K_t obtained from the Angremond et al. [25] and Van Der Meer et al. [26] (**Error! Reference source not found.**c, d), but it also has a slight difference in statistical parameters, as described in Table 3. The best statistical performance was obtained from van der Meer's formula with adjusted R-squared, R^2=0.88, *MSE*=0.0028, and *RMSE*=0.053. Because this equation is in general form, it can be applied to many types of breakwaters and can explain 88% experimental data. The following linear equation with statistical performance is R^2=0.82, *MSE*=0.0033, and *RMSE*=0.058. The next one is d'Angremond's et al. [25] formula with R^2=0.78, *MSE*=0.0041, and *RMSE*=0.064. This formula applied for pile-rock breakwater is best fit with a range of -0.5 < $R_c/H_{m0,i}$ < 0.3. and not highly suitable for a range of -0.5 < $R_c/H_{m0,i}$ < 2.0. Therefore, for d'Angremond's formula, it can be applied for submerged breakwater. However, for d'Angremond's formula, it can be applied to the submerged breakwater. So this formula may not be used for

 doi:10.20944/preprints202210.0433.v1

the emerged breakwater. The non-linear equation yields a lower value of adjusted R-squared (R^2) compared to the three equations mentioned above, with R^2=0.73, MSE=0.0044, and $RMSE$=0.066 (see **Error! Reference source not found.**). However, non-linear equation is valuable because this can fit well in a range of $0 < R_c/H_{m0,i} < 2$ while linear equation unable to fit this range corresponding to the breakwater working condition in submerged or semi-submerged states ($R_c \leq 0$). This study confirms that our developed formulas are suitable for Pile-rock breakwater with linear and non-linear equations. This experiment also provides a data set for further studies with the investigation of different types of formulas for breakwaters.

In order to define the suitability of previous formulas developed by Le Xuan et al. [11], Tuan & Luan [27],and Tuan et al. [28] for PRBW, we have calculated K_t from these equations and evaluated the statistical indices as following. Both formulas from [27, 28] yield very low adjusted R-squared values and relative high MSE and $RMSE$ with values R^2=0.04, MSE=0.0224, $RMSE$=0.150, and R^2=0.22, MSE=0.0285, $RMSE$=0.169, respectively (see **Error! Reference source not found.**). This means that these formulas should not be applied for Pile-rock breakwater. Therefore, we recommend not applying these equations for PRBW. The K_t obtained from the formula of Le Xuan et al. [11] is highly similar to experimental data and this study but not so high with R^2=0.61, MSE=0.0086, RMSE=0.093 because of the same structure of Pile-rock breakwater. Nonetheless, Le Xuan et al. [11] equation can explain 61% experimental data while our equations can explain from 73% to 82% of experimental data.

Table 3. Statistical performance of various formulas from different studies.

Empirical equations	R^2	MSE	RMSE
van der Meer et al. (2005)	0.88	0.0028	0.053
d.Angremond et al. (1996)	0.78	0.0041	0.064
Linear equation	0.82	0.0033	0.058
Non-linear equation	0.73	0.0044	0.066
Tuan et al. (2018)	0.04	0.0224	0.150
Tuan & Luan. (2020)	0.22	0.0285	0.169
Le Xuan et al. (2020)	0.61	0.0086	0.093

Note: R^2 is adjusted R-squared, $R^2 = 1 - (MS_{error}/MS_{total})$, MS_{error}: mean square due to error, MS_{total}: mean square total

Preprints (www.preprints.org) | NOT PEER-REVIEWED | Posted: 27 October 2022 doi:10.20944/preprints202210.0433.v1

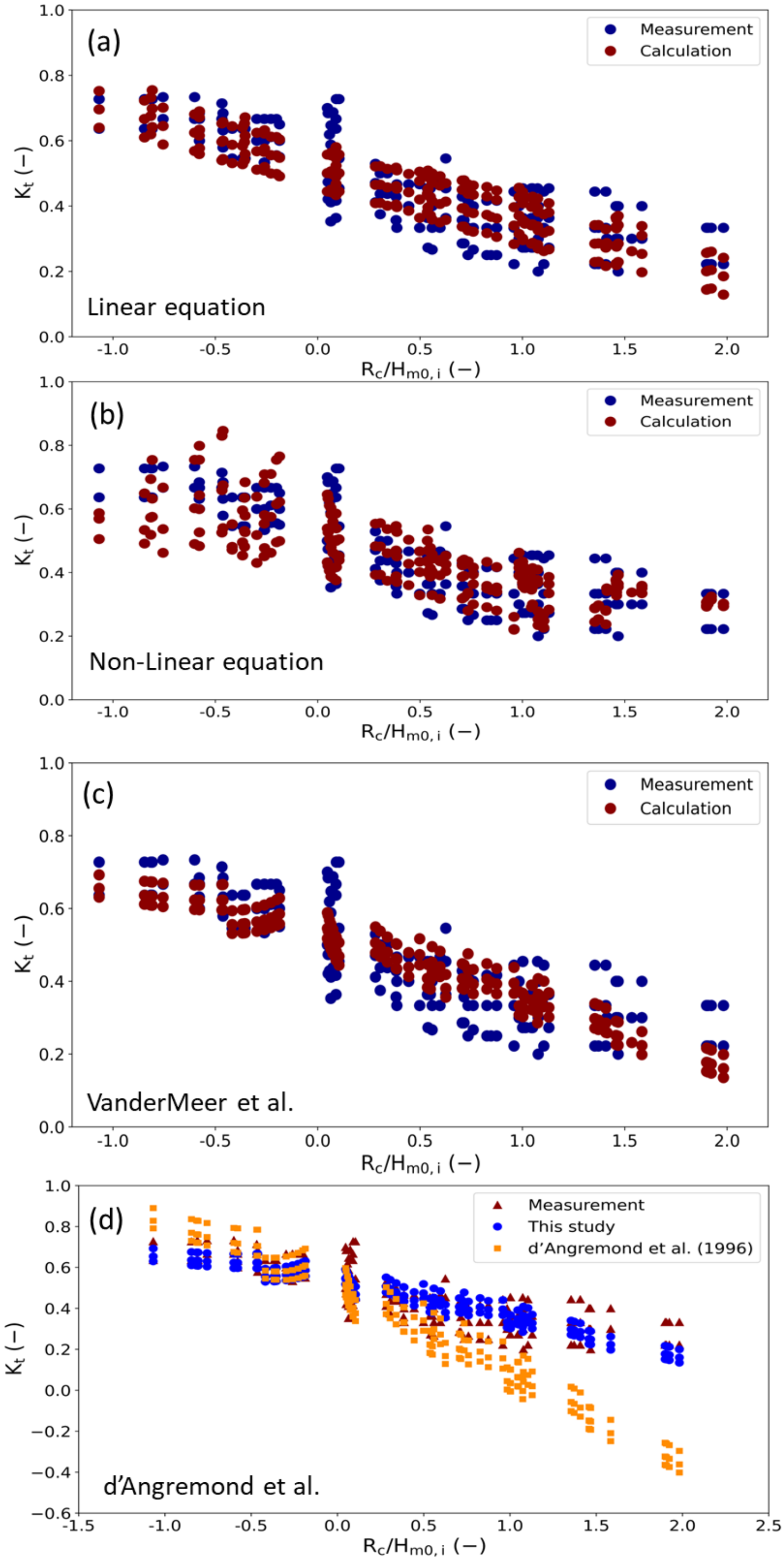

Figure 19. The comparison of K_t against the relative crest freeboard by different empirical equations.

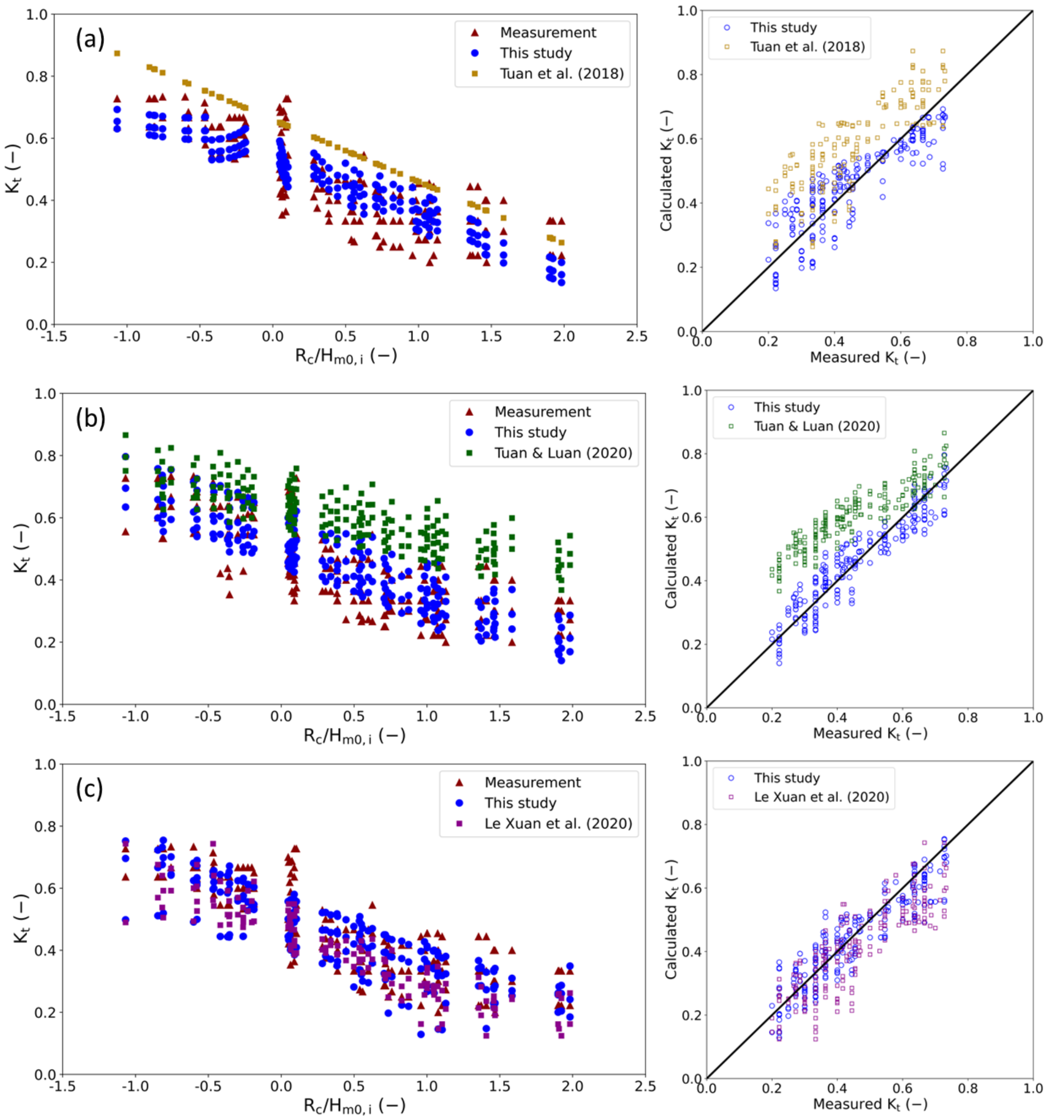

Figure 20. The correlation of K_t and relative crest freeboard and scatter plots obtained from different formulas compared with our study.

Error! Reference source not found. shows the comparison of the correlation of K_t and relative crest freeboard and scatter plots between previous studies carried out by Le Xuan et al. [11], Tuan & Luan [27],and Tuan et al. [28] with the current study. The K_t of Tuan et al. [28] (**Error! Reference source not found.**a left) decreases over time as $R_c/H_{m0,i}$ increases over time, and these values are found to be larger than the measurement data as well as the values in the current study (**Error! Reference source not found.**a right). The reason is that the porosity of the perforated hollow breakwater is very large, which leads to high wave energy transmitted through the breakwater. In the study of Tuan and Luan. [27] experimented with the bamboo fence permeable breakwater, the values of the K_t also tend to decrease over time when $Rc/H_{m0,i}$ increases (**Error! Reference source not found.**b, left). However, most of the K_t values are overestimated compared to this study and measurement values (**Error! Reference source not found.**b, right). Because the Bamboo fence was built using bamboo poles and brushwood bundles which have very low wave resistance. Therefore, the wave energy transmission capacity is very high. **Error! Reference source not found.**c shows that the value of K_t is similar to those in Le Xuan et al. [11] because the breakwater in this study has the same structural shape as [11]. The centrifugal piles and rock inside could significantly dissipate the wave energy compared to those by [27, 28].

4. Conclusions

The experiments evaluated the effect of PRBW width on the wave transmission, reflected, and energy dissipation coefficients which were performed on the 2D physical model in a wave flume. The results show a significant influence of crest width dimensions on the wave energy coefficients. This study has developed a correlation between the parameters that govern the efficiency of wave reduction, wave reflection, and wave energy dissipation. The results show that the crest width of the breakwater is inversely proportional to the wave transmission coefficient (K_t) and shows a clear tendency under emerged state. The crest width of the breakwater is directly proportional to the wave reduction efficiency and wave energy dissipation capacity of the breakwater in all working states (submerged and emerged states). The crest width has also influenced the wave reflection coefficient. The incident wave disturbance coefficient in front of the structure is proportional to the reflected wave coefficient, and the wave in front of the structure can increase the height by 1.4 times in the emerged state. The results of this study serve as the basis for the PRBW design to enhance the efficiency under different natural conditions in the coastal Mekong Delta. The findings of the study are necessary to be considered for structural stability analysis of breakwater in the nearshore wave condition. Moreover, this study also developed the empirical formulas and compared the wave transmission coefficients with previous studies with different types of breakwaters. The empirical equations could be useful for designing tasks without relying on physical experiments.

Author Contributions: Conceptualization, Nguyet-Minh.N. and Duong.D.V., Tu.L.D.; methodology, Duong.D.V., Tu.L.D., Duong.T.A.; software, Tu.L.D., Truong.P.N., Phong.N.T.; validation, Nguyet-Minh.N. Duong.T.A.; formal analysis and data curation, Tu.L.D., Truong.P.N., Phong.N.T.; investigation and resources, Duong.D.V. and Tu.L.D., Nguyet-Minh.N; writing—original draft preparation, Nguyet-Minh.N., Duong.T.A., Thanh.D.D., Ahad.H.T.; writing—review and editing, Nguyet-Minh.N, Duong.T.A, Thanh.D.D, Ahad.H.T; visualization, Tu.L.D., Truong.P.N, Phong.N.T; supervision and project administration, Duong.T.A. and Nguyet-Minh.N.; funding acquisition, Nguyet-Minh.N. All authors have read and agreed to the published version of the manuscript.

Funding: The research work described herein was funded by the Ministry of Science and Technology (MOST) in the national project (No. ĐTĐL.CN-47/18) "Physical model experiment for investigating coastal protection measures of Mekong Delta."

Institutional Review Board Statement: Not applicable

Informed Consent Statement: Not applicable

Data Availability Statement: The datasets generated during and/or analyzed in this study are available from the corresponding author upon reasonable request.

Acknowledgments: Many thanks to the Southern Institute of Water Resources Research for providing all data, model licenses, and necessary information. The authors greatly appreciate the Editor and sincerely thank the three anonymous reviewers for their constructive comments to improve the manuscript.

Conflicts of Interest: Authors The authors declare no conflict of interest. The funders had no role in the design of the study; in the collection, analyses, or interpretation of data; in the writing of the manuscript; or in the decision to publish the results.

References

1. Kondolf, G. M., Rubin, Z. K., & Minear, J. T. Dams on the Mekong: Cumulative sediment starvation. *Water Resour. Res.* **2014**, *50*, 5158-5169.
2. Kondolf, G. M., Annandale, G. E. O. R. G. E., & Rubin, Z. Sediment starvation from dams in the lower Mekong river basin: magnitude of the effect and potential mitigation opportunities. In E-proceedings of the 36th IAHR World Congress, 28 June – 3 July, 2015, Hague, Netherlands.
3. Minderhoud, P. S. J., Coumou, L., Erkens, G., Middelkoop, H., & Stouthamer, E. Mekong delta much lower than previously assumed in sea-level rise impact assessments. *Nat. Commun.* **2019**, *10*, 1-13.

Preprints (www.preprints.org) | NOT PEER-REVIEWED | Posted: 27 October 2022 doi:10.20944/preprints202210.0433.v1

4. Le Xuan, T., Thanh, V.Q., Reyns, J., Van, S.P., Anh, D.T., Dang, T.D. and Roelvink, D. Sediment transport and morphodynamical modeling on the estuaries and coastal zone of the Vietnamese Mekong Delta. *Cont. Shelf Res.* **2019**, *186*, pp.64-76.
5. Thanh, V. Q., Reyns, J., Wackerman, C., Eidam, E. F., & Roelvink, D. Modelling suspended sediment dynamics on the subaqueous delta of the Mekong River. *Cont. Shelf Res*. **2017**, *147*, 213-230.
6. Van Manh, N., Dung, N. V., Hung, N. N., Kummu, M., Merz, B., & Apel, H. Future sediment dynamics in the Mekong Delta floodplains: Impacts of hydropower development, climate change and sea level rise. *Glob. Planet. Change*. **2015**, *127*, 22-33.
7. Erban, L. E., Gorelick, S. M., & Zebker, H. A. Groundwater extraction, land subsidence, and sea-level rise in the Mekong Delta, Vietnam. *Environ. Res. Lett*. **2014**, *9*, 084010.
8. Dang, T. D., Cochrane, T. A., & Arias, M. E. Future hydrological alterations in the Mekong Delta under the impact of water resources development, land subsidence and sea level rise. *J. Hydrol. Reg. Stud*. **2018**, *15*, 119-133.
9. Albers, T., San, D. C., & Schmitt, K. Shoreline management guidelines: Coastal protection in the Lower Mekong Delta. *Dtsch. Ges. Für Int. Zs.(GiZ) GmbH Manag. Nat. Resour. Coast. Zone Soc Trang Prov*. **2013**, *1*, 1-124.
10. Tran, V. T., Nguyen, H. H., Pham, D. H., Nguyen, D. N., & Nguyen, T. T. Hollow cylinder breakwater for dissipation of wave energy to protect the west coast of Ca Mau Province in Vietnam. In Proceedings of the 1st Vietnam Symposium on Advances in Offshore Engineering, 1–3 November 2018, Hanoi, Vietnam
11. Le Xuan, T., Ba, H.T., Le Manh, H., Do Van, D., Nguyen, N.M., Wright, D.P., Bui, V.H., Mai, S.T. and Anh, D.T. Hydraulic performance and wave transmission through pile-rock breakwaters. *Ocean Eng*. **2020**, *218*, 108229.
12. Nguyen, T. P., Van Tam, N., & Parnell, K. E. Community perspectives on an internationally funded mangrove restoration project: Kien Giang province, Vietnam. *Ocean Coast Manag*. **2016**, *119*, 146-154.
13. Nguyen, T. P., & Parnell, K. E. Gradual expansion of mangrove areas as an ecological solution for stabilizing a severely eroded mangrove dominated muddy coast. *Ecol. Eng*. **2017**, *107*, 239-243.
14. Luom, T. T., Phong, N. T., Anh, N. T., Tung, N. T., Tu, L. X., & Duong, T. A. Using Fine-Grained Sediment and Wave Attenuation as a New Measure for Evaluating the Efficacy of Offshore Breakwaters in Stabilizing an Eroded Muddy Coast: Insights from Ca Mau, the Mekong Delta of Vietnam. *Sustainability*. **2021**, *13*(9), 4798.
15. Nhan, N. H. Assessing the impact of embankment to create beach in the west coast of Ca Mau province. *J of Irri. Sci. Tech*. **2013**, *17*, 4-18 (in Vietnamese)
16. Nguyen, H.H. and Duong, C.M., 2019, September. Stability analysis of a double-row pile breakwater subjected to combined loading in Mekong Delta. In Proceedings of the 10th International Conference on Asian and Pacific Coasts (APAC 2019) Hanoi, Vietnam, 25-28 September 2019
17. Hur, D. S. Deformation of multi-directional random waves passing over an impermeable submerged breakwater installed on a sloping bed. *Ocean Eng*. **2004**, *31*, 1295-1311.
18. Hur, D. S., Lee, K. H., & Choi, D. S. Effect of the slope gradient of submerged breakwaters on wave energy dissipation. *Eng. Appl. Comput. Fluid Mech*. **2011**, *5*, 83-98.
19. Tsai, C. P., Chen, H. B., & Lee, F. C. Wave transformation over submerged permeable breakwater on porous bottom. *Ocean Eng*. **2006**, *33*, 1623-1643.
20. Lin, P., & Karunarathna, S. A. Numerical study of solitary wave interaction with porous breakwaters. *J. Waterw. Port, Coast. Ocean Eng*. **2007**, *133*, 352-363.
21. Zhang, J. S., Jeng, D. S., & Liu, P. F. Numerical study for waves propagating over a porous seabed around a submerged permeable breakwater: PORO-WSSI II model. *Ocean Eng*. **2011**, *38*, 954-966.
22. Wu, Y. T., & Hsiao, S. C. Propagation of solitary waves over a submerged permeable breakwater. *Coast. Eng*. **2013**, *81*, 1-18.
23. Wu, Y. T., Yeh, C. L., & Hsiao, S. C. Three-dimensional numerical simulation on the interaction of solitary waves and porous breakwaters. *Coast. Eng*. **2014**, *85*, 12-29.
24. Van der Meer, J. W., & Daemen, I. F. Stability and wave transmission at low-crested rubble-mound structures. *J. Waterw. Port, Coast. Ocean Eng*. **1994**, *120*, 1-19.
25. d'Angremond, K., Van Der Meer, J. W., & De Jong, R. J. Wave transmission at low-crested structures. *Coast. Eng*. **1996**, 2418-2427
26. Van der Meer, J.W., Briganti, R., Zanuttigh, B. and Wang, B. Wave transmission and reflection at low-crested structures: Design formulae, oblique wave attack and spectral change. *Coast. Eng*. **2005**, *52*, 915-929.
27. Tuan, T.Q. and Luan, M.T. Monsoon wave transmission at bamboo fences protecting mangroves in the lower mekong delta. *Appl. Ocean Res*. **2020**, *101*, 102259.
28. Tuan, T.Q., San, D.C., Tu, L.X., Duong, D.V. Research on the wave reduction efficiency of perforated hollow breakwater on the wave flume. *J. Hydraul. Res*. **2018**, *49*, 109 (in Vietnamese)